

Electromagnetic ELM and inter-ELM filaments detected in the COMPASS Scrape-Off Layer



M. Spolaore^{a,*}, K. Kovařík^{b,c}, J. Stöckel^b, J. Adamek^b, R. Dejarnac^b, I. Ďuran^b, M. Komm^b, T. Markovic^{b,c}, E. Martines^a, R. Panek^b, J. Seidl^b, N. Vianello^a, the COMPASS team

^a Consorzio RFX, Corso Stati Uniti 4, 35127 Padova, Italy

^b Institute of Plasma Physics AS CR, Za Slovankou 3, Prague, Czech Republic

^c Faculty of Mathematics and Physics, Charles University in Prague, Czech Republic

ARTICLE INFO

Article history:

Received 15 July 2016

Revised 25 November 2016

Accepted 13 December 2016

Available online 29 December 2016

Keywords:

Electromagnetic filaments

ELMs

Scrape-Off Layer

Magnetic fluctuations

Current density

ABSTRACT

In fusion devices strong interest is deserved to the edge filament transport both related to turbulent and ELM structures, because they are believed to provide important interaction with the plasma facing components and divertor plates. Among their features also the electromagnetic (EM) properties are expected to play an important role and in particular for the high beta regimes expected in future devices. The presence of ELM and inter-ELM electromagnetic filaments were detected during H-mode discharges in COMPASS device Scrape-Off Layer, where a new probe head was recently developed and commissioned. The diagnostic allows the simultaneous measurements of electrostatic and magnetic fluctuations with high time resolution, suitable for the identification of EM features of filaments. The method allows in particular the direct measurement of the current density associated to filaments. Detailed electrostatic and electromagnetic features analysis revealed a complex and fragmented structure within a single ELM and strong peaks in parallel current density J_{tor} are observed to characterize the ELM bunch. Analogous EM structures are observed also in inter-ELM phase, but with more than one order of magnitude lower intensity and time scale.

© 2017 Elsevier Ltd.

This is an open access article under the CC BY-NC-ND license.

(<http://creativecommons.org/licenses/by-nc-nd/4.0/>)

1. Introduction

Filamentary structures have been observed in all magnetic configurations with very similar features despite the difference in the magnetic geometry, they are magnetic-field aligned plasma structure considerably denser than the surrounding plasma and localized on the cross-field plane. Theory and experiments suggest these filament or blobs exhibit a radial convective motion across the Scrape-Off Layer (SOL), and the interest in blob dynamics is further motivated by their interaction with first wall and divertor. Indeed by increasing particle and heat flux into the far SOL, blobs can increase interaction with limiters, RF antennas and first wall [1].

It is interesting to note that, despite their possible different generation mechanism, blobs and Edge Localized Mode (ELM) filaments [2] share some common physical features, as the above mentioned localization in the perpendicular plane and the associ-

ated parallel current, with a convective radial velocity components somehow related to their dimension [3,4]. Interestingly, the role of these turbulent eddies in providing substantial sheared flow in the external region has been recently considered as important in the process of LH transition [5,6]. Actually, since the vorticity drive provided by turbulent eddies gets stronger as heating power is increased, it should naturally lead to a very strong shear flow, which can ultimately lead to an H-Mode whether heating is enough. A further fundamental aspect of blob studies needs to be deeply investigated, namely the electromagnetic (EM) effects on filaments [7]. These studies, only recently addressed from the experimental point of view [8–10] deserve additional effort, in particular for the implication they could have for ELM filaments. On the one hand, it is supposed, and experimentally observed, that at enough high beta, blobs can transport current, and the role of these current in ELM filaments dynamics is still an open issue. On the other hand at enough high beta blobs can also carry “frozen in” magnetic field lines, with the possibility of causing line bending which could enhance the interaction of blobs with the first wall, without letting those blob to hit divertor plates [1]. Another still unan-

* Corresponding author.

E-mail address: monica.spolaore@igi.cnr.it (M. Spolaore).

swered question regards the dynamics of blobs/filaments in the transition region between closed and open field lines. This issue could also include the interaction of such structures with applied magnetic perturbation, as foreseen in Resonant Magnetic Perturbation technique (RMP), which breaks the 2D symmetry with the appearance of a 3D topology with the stable and unstable manifolds of the separatrix. Thus detailed comprehension of generation mechanism, dynamics and characteristic of filaments represents a fundamental physical issue for both present and future devices.

In this contribution the presence of ELMs and inter-ELM EM filaments will be investigated on their EM features in the COMPASS tokamak, where a new probe head was recently developed and successfully commissioned [11].

The diagnostic, based on the U-probe concept [12], allows the simultaneous measurements of electrostatic and magnetic fluctuations, with high time resolution suitable for the identification of EM features of filaments, providing in particular the direct measurement of the current density associated to filaments. The probe head was inserted in the SOL of D-shaped diverted discharges. The COMPASS experiment was operated in these discharges in ohmic and NBI assisted H-mode, with the clear presence of different type of ELMs.

The paper is organized as follows. In Section 2 the main features of the COMPASS tokamak are described with the specific edge diagnostic and methods used in this paper, in Section 3 the general features of a typical NBI ELMy H-mode discharge are shown, in Sections 4 and 5 the fine electrostatic and electromagnetic (EM) features detected respectively on ELM and inter-ELM filaments in the same discharge are described, in the last session some conclusions are drawn.

2. Experimental setup and method

The COMPASS tokamak [13] is a compact experimental device ($R = 0.56$ m, $a = 0.2$ m) operated in divertor plasma configuration with ITER-like plasma cross-section. The vacuum vessel of COMPASS is equipped with an open divertor covered by carbon tiles. Presently, COMPASS operates with plasma current up to 400 kA and toroidal magnetic field in the range 0.9–1.8 T and elongation up to 1.8. The data shown in this paper refer to $I_p = 300$ kA and $B_t = 1.15$ T, D-shaped plasmas in Single Null (SN) configuration with the ion grad-B drift direction towards the X-point, see the poloidal section shown in Fig. 1.

Two neutral beam injectors provide nominal power of 2×0.4 MW at the beam energy of 40 keV for additional plasma heating. Ohmic as well as NBI assisted H-mode have been successfully achieved on the COMPASS tokamak after application of boronization of the vacuum vessel interior. The L–H power threshold PLH has a minimum at line-average density in the range of $3.5\text{--}4 \times 10^{19} \text{ m}^{-3}$. The L–H transition is followed either by an ELM-free period or ELMs with frequency in the range of 80–1000 Hz.

In this paper the case of type-I ELMs will be analyzed focusing on one representative discharge (#9334), where the NBI assisted H-mode was obtained. The edge measurements presented in this paper are mainly provided from a specifically developed insertable probe head and described in [10], the COMPASS U-probe. This diagnostics is based on the U-probe concept [8,11] and allows the simultaneous measurements of electrostatic and magnetic fluctuations, with high time resolution suitable for the identification of EM features of filaments, providing in particular the direct measurement of the current density associated to filaments. The probe, see Fig. 1, is based on two identical towers poloidally spaced by 40 mm covered by a BN case, each of them equipped with 6 lateral electrostatic pins radially spaced by 6 mm, and three pins on top. Inside the case are located three 3-axial magnetic pickup coils. They are arranged to form a 2D configuration among the two tow-

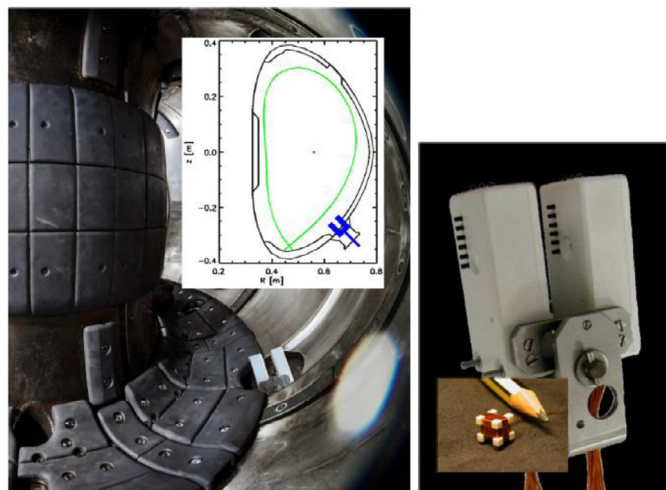


Fig. 1. Inner view of the COMPASS camera with the porthole where the probe head was inserted is shown. The scheme of the probe poloidal section with the LCFS in green is shown in the inner square. Picture on the right shows the U-probe for COMPASS experiment and the detail of the pick-up coils equipping the probe. (For interpretation of the references to colour in this figure legend, the reader is referred to the web version of this article.)

ers, lying on the cross-field plane. The concept would allow the direct estimate of the parallel current density fluctuation estimate from the Ampere's law $J_{\text{par}} = (\nabla \times B)_{\text{par}} / \mu_0$, where B is the local average magnetic field.

This method represents a simplified 2D version of the one adopted in the Cluster mission for the measurement of currents in the magnetosphere [14] and was applied for the first time in a fusion experiment in RFX-mod [15]. All signals are acquired with a 5Ms/s acquisition frequency. The probe is inserted in the SOL region from the port on the bottom part of the machine, as shown in Fig. 1. Its radial position can be modified on a shot-to-shot basis.

The COMPASS tokamak is also equipped with one array of 39 Langmuir probes (LP) in the divertor region, their poloidal spatial resolution is about 5 mm [16,17]. The divertor sensor system is completed by an array constituted by 10 Ball Pen Probes (BPP) and 4 additional LPs and placed in the toroidal opposite side of the machine [12,18].

3. ELMy H-mode discharges in COMPASS tokamak

An example of discharge with a long lasting H-mode transition is shown in Fig. 2, where some general plasma signals for the shot #9334 are represented.

In this case a flattop plasma current I_p of about 300 kA was obtained, with an edge safety factor $q_{95} \sim 2.5$ and a central density $n_e \sim 6 \times 10^{19} \text{ m}^{-3}$. In this shot additional heating was applied through the NBI system operating in the time window from 1100 to 1200 ms with ~ 190 kW injected power. The transition to the H-mode is clearly visible after $t = 1065$ ms, where a sudden drop of the D_α signal is observed as well as an abrupt increase of the core density. It can be also observed that huge peaks in the D_α signal characterize the H-mode phase. Those strong events are commonly [19] associated to the ELM filaments interacting with the first wall. Most of the time during the H-mode phase, their occurrence frequency is relatively low, of the order of 250 Hz increasing up to 500 Hz in the time window from 1090 and 1110 ms, corresponding to a main density decrease. According to the classification described in [20] these events are identified in COMPASS as type-I ELMs.

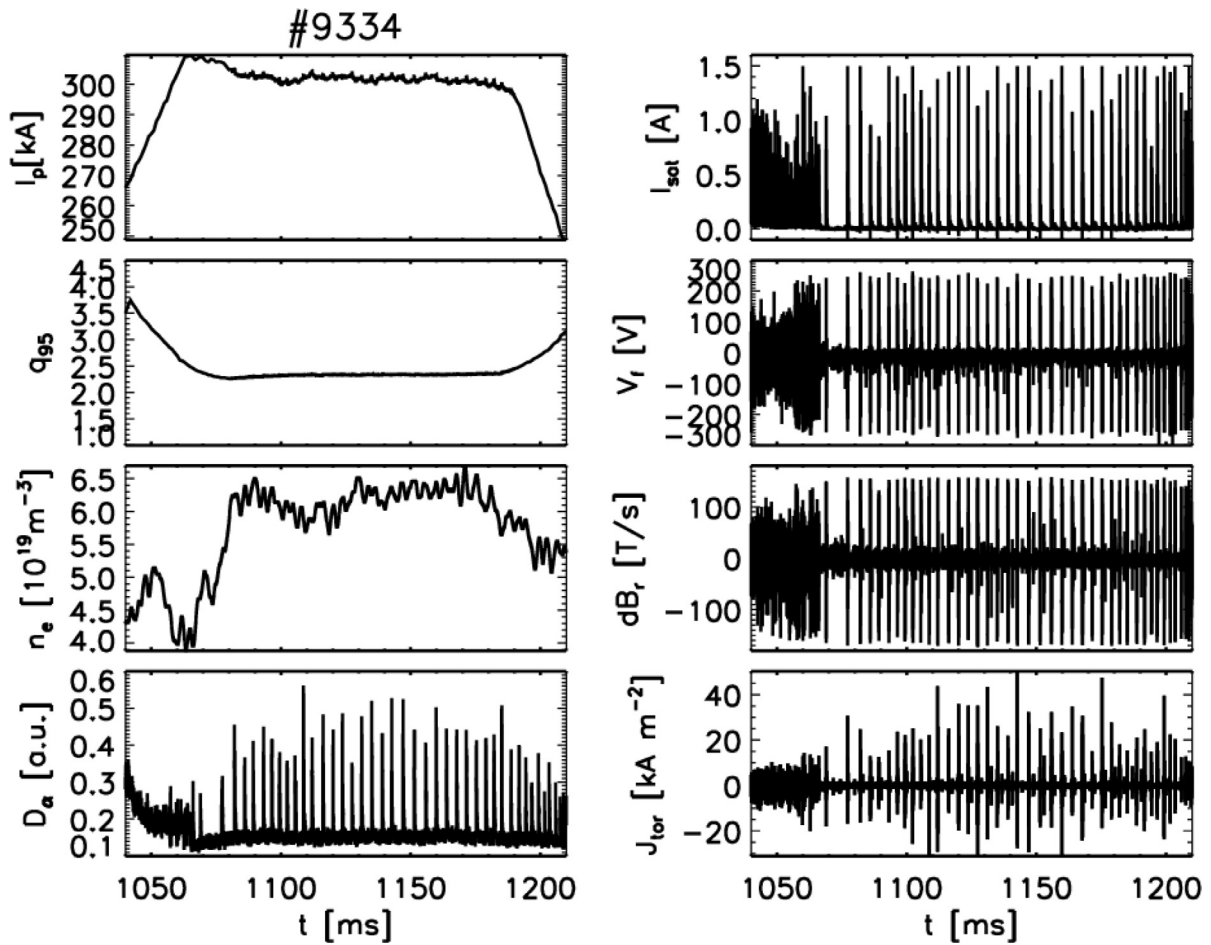


Fig. 2. Example of an H-mode shot (#9334) obtained with NBI additional heating (~ 190 kW from 1100 to 1200). Left column shows some general shot signals: plasma current, q_{95} , plasma density, D_α . Right column shows some representative electrostatic and magnetic signals obtained from the COMPASS U-probe.

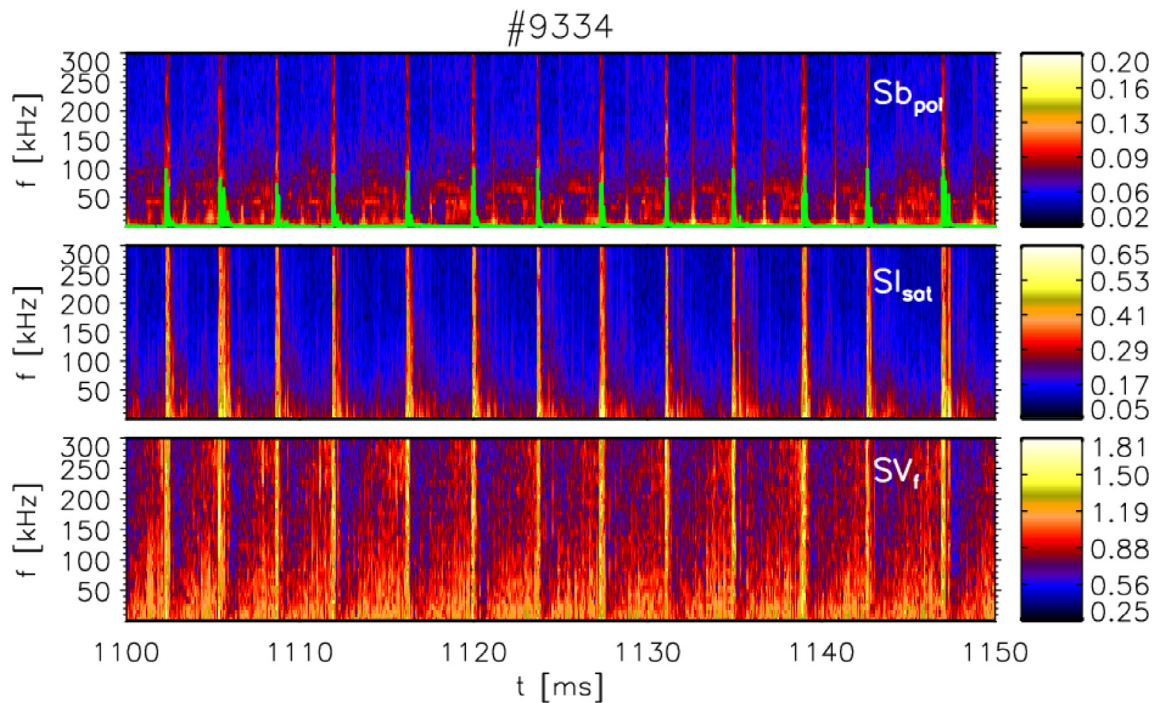


Fig. 3. Top panel: spectrogram of the poloidal component of magnetic field fluctuation ($S_{b_{\text{pol}}}$) during the H-mode phase, in green the I_{sat} local measure in a.u. is over-plotted for comparison. Central and bottom panels: spectrogram ($S_{I_{\text{sat}}}$) of the local I_{sat} and spectrogram (S_{V_r}) of the local V_r in the same time window. Measures provided by the COMPASS U-probe. (For interpretation of the references to colour in this figure legend, the reader is referred to the web version of this article.)

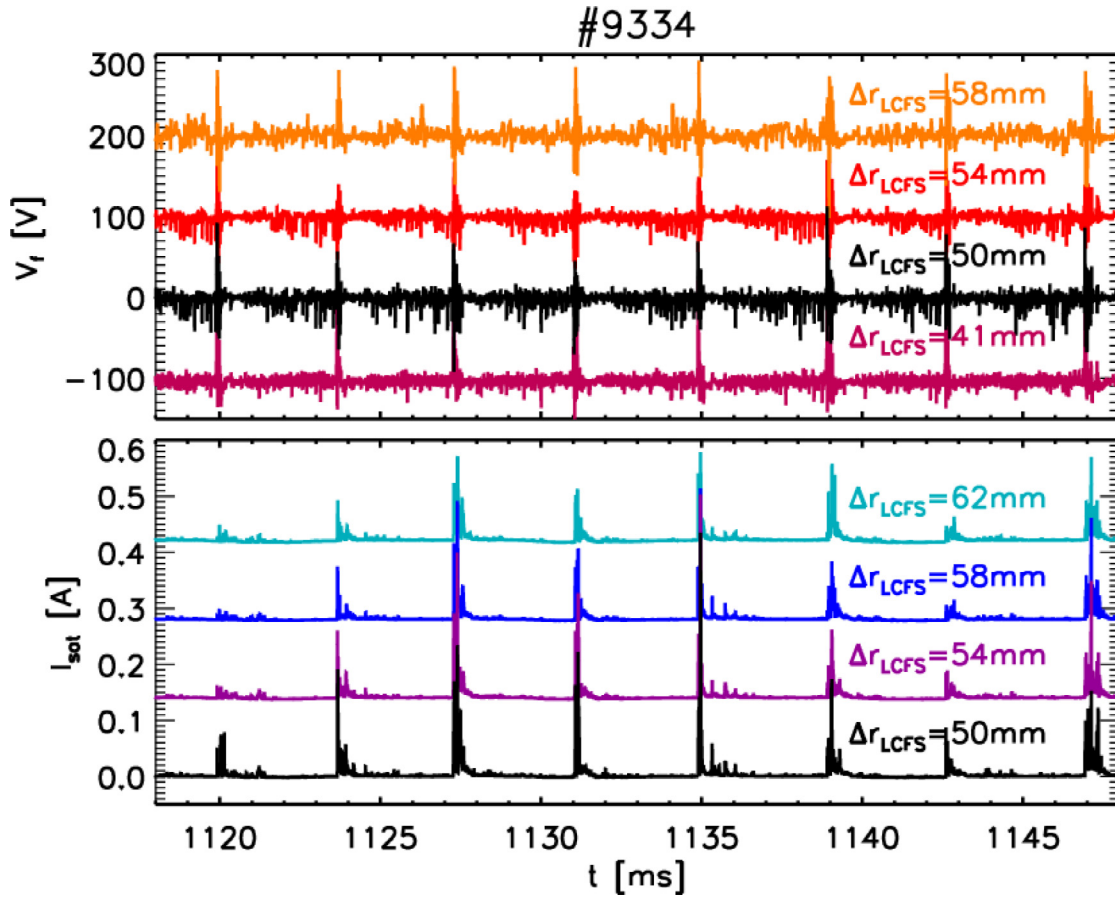


Fig. 4. Top panel: Time evolution during ELMy H-mode of the floating potential measured at four different radial positions with respect to the LCFS. Bottom panel: the same for I_{sat} measurements. (For interpretation of the references to colour in this figure legend, the reader is referred to the web version of this article.)

Fig. 2 shows also some representative electrostatic and magnetic signals provided by the COMPASS U-probe. In particular the ion saturation current, I_{sat} , indicative of the local plasma density value and the floating potential, V_f , were measured in the most inserted position available at one of the probe towers. For the shot 9334, the U-probe was inserted at 15 mm depth from the first wall, corresponding to a position of approximately 50 mm radially outside from the estimated local radial position of the Last Closed Flux Surface (LCFS), see the Fig. 1 insert.

It can be observed that the I_{sat} signal as well exhibits, during the H-mode phase, huge peaks. Those are indication of strong density burst and clearly associated to the ELM events observed in the D_α signal. On the other hand also the local V_f exhibits events with the same periodicity, in particular in this case V_f bursts are generally dipolar, i.e. a roughly double structure, positive and negative peak, appears associated to each event. A more detailed analysis of this behavior will be presented in the next paragraphs. As representative of magnetic signals, the time behavior of the radial component db_r/dt fluctuations is shown together with the corresponding evaluation of the local cross-field current density fluctuations, δJ_{tor} . The δJ_{tor} was evaluated via the cross-field circuitation and strong events related to the ELMy behavior are very well identified. The time evolution of the δJ_{tor} with strong peaks corresponding to D_α events provides a clear indication of the electromagnetic features of these ELMs.

More detail on this aspect can be found in Fig. 3, where a spectrogram of the poloidal magnetic field fluctuation, δb_{pol} , is shown as a matter of example during the type-I ELM phase. The signal of I_{sat} is chosen as trigger identification of the presence on the probe

location of an ELM occurrence. To this end the I_{sat} signal, green line in the top panel of Fig. 3, is overlapped to the δb_{pol} fluctuation spectrogram (Sb_{pol}). It can be observed that each one of the I_{sat} burst corresponds to a strong peak in the magnetic spectrogram involving all the explored frequencies. This abrupt frequency spreading on the magnetic activity indicates that a magnetic structure localized in time is associated to these events. In the inter-ELM phases the power spectrum level is strongly reduced, however some features can be highlighted. In particular one additional spectrum spreading burst is observed in each inter-ELM phase but with much lower intensity and not correlated to the occurrence of local I_{sat} strong peaks. It is worth mentioning that they are instead well correlated to the Soft X-ray radiation drops and related to sawtooth activity, see also Section 5. In addition a systematic discrete mode magnetic activity is observed, in the frequency range 50–150 kHz, in the phase preceding the ELM occurrence and disappearing right after. Analogous features are detected in all the three component of the magnetic field fluctuations.

The spectrogram was calculated in the same time window also for the electrostatic quantities V_f and I_{sat} . The I_{sat} signal spectrogram is shown in the middle panel of Fig. 3. The abrupt spreading of spectrum at the I_{sat} ELMy bursts is visible as in the magnetic fluctuations, indicating the presence of a spatially localized structure at the ELM event occurrence. In the inter-ELM phase a series of spectrogram spreading events follow the ELM time occurrence, with a generally decreasing intensity. On the other side no evidence of discrete modes in the inter-ELM phase of the I_{sat} spectrogram is detected and the fluctuations are very low in the phase preceding the ELM. In the V_f spectrogram (Fig. 3 bottom panel)

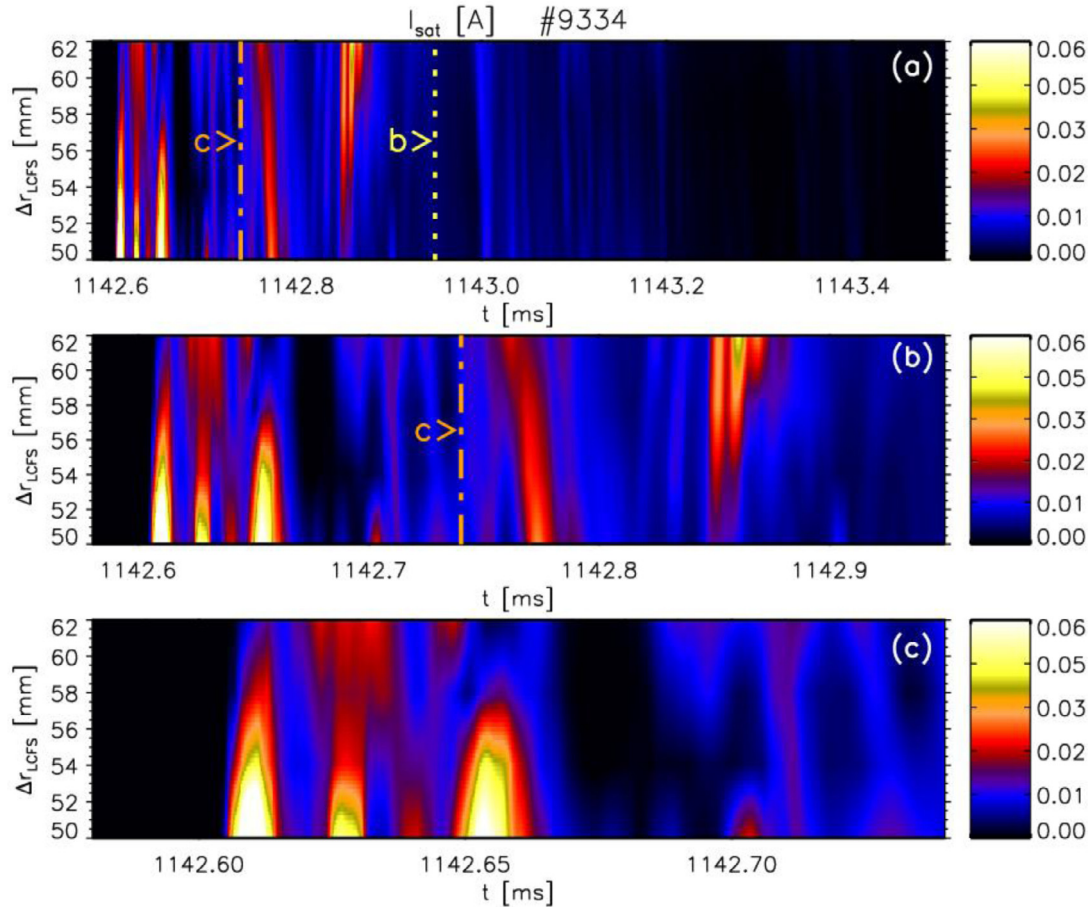


Fig. 5. Time evolution of the local $I_{\text{sat}}(\Delta r_{\text{LCFS}}, t)$ radial profile, obtained from the I_{sat} signals shown in Fig. 4, during one single ELM. From (a) to (c) increased zoom details are shown. Dashed vertical lines and labels 'b >' and 'c >' indicate the latest times/time considered in the below panels/panel. (For interpretation of the references to colour in this figure legend, the reader is referred to the web version of this article.)

the bursty spreading at the ELM occurrence is detected as well. In this case, differently from I_{sat} , a wide spread activity is present also in the inter-ELM phase, involving the whole explored frequency range, so that coherent modes if any are not clearly apparent as in the magnetic fluctuations case. Further details on inter-ELM phase will be shown in Section 5.

4. ELM fine structure

4.1. Electrostatic features and radial behavior

Information on the event features along the radial direction can be obtained by exploiting the radially distributed electrostatic pins in the COMPASS U-probe. An example is shown in Fig. 4, where the radial array on one tower was configured for I_{sat} measurements, while the array on the other tower measured V_f and I_{sat} alternately. In the top panel of Fig. 4 the time evolution of V_f signals measured at four different distances $\Delta r_{\text{LCFS}} = r - r_{\text{LCFS}}$ is shown, where r_{LCFS} is the LCFS closest position to the probe head location and r is the measurement radial position. In particular $\Delta r_{\text{LCFS}} > 0$ indicates positions outside the separatrix. The same ELM-phase time window of Fig. 3 is considered. The behavior of V_f signals is analogous to the one shown in the example of Fig. 2, it is confirmed that both positive and negative strong peaks are associated to the ELM occurrence and this behavior is replicated with different intensities along the radial direction. It can then be concluded that the ELM V_f structure involves all the radially distributed pins in the probe head, indicating a radial extension covering at least

the 4 cm monitored by the probe. Analogous considerations can be deduced from the radial array of I_{sat} measurements, even if performed in a different tower poloidally spaced by 4 cm. The four I_{sat} signals, in the bottom panel of Fig. 4, indicate a bursty behavior at the ELM occurrence involving all the probe location measurements. A series of generally decreasing intensity peaks are observed right after the first huge one, see also [17], and this fine behavior with strong and weaker events are well replicated along the radial direction. These features suggest a more complex structure in the density behavior and this can be analyzed by zooming on one single ELM event. Fig. 5 shows the time evolution during a single event of the density fluctuation radial profile at the probe head location. Profiles are obtained in this case from the four I_{sat} signals, radially spaced by 4 mm, shown in Fig. 4. Measurements are plotted as a function of Δr_{LCFS} . The three panels of figure show increasing detailed time behavior around a single one event. It can be observed that the apparent single burst in I_{sat} signals examined in Fig. 2 is composed by radially extended multiple bursts. Furthermore some density fragments appear tilted in the radial-time plane. In other words a certain delay is observed between I_{sat} burst in the most inserted and outer pins, and in this case an outward radial propagation velocity can be derived. In particular for the data shown in Fig. 5 (bottom panel) where the time scale allows distinguishing few radial propagating density fragments, a radial velocity of the order of 1 km/s can be estimated. As a matter of comparison, radial velocities of ~ 8 km/s were measured by the Gas Puffing Imaging for ELM filaments ejected in the SOL of NSTX [21]. So that the ELM density structure, confirming the indication

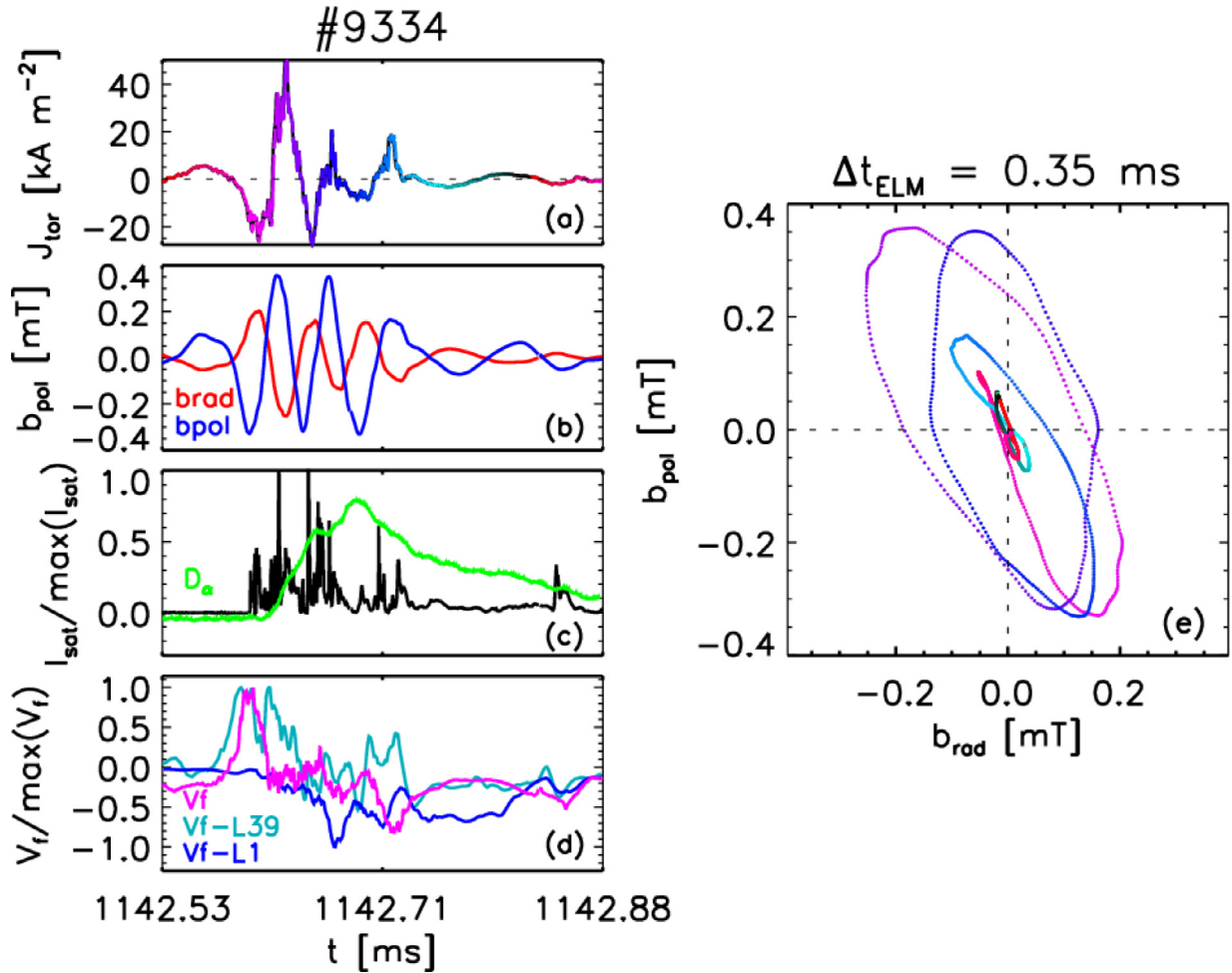


Fig. 6. Time evolution around a single ELM occurrence of the (a) δJ_{tor} , (b) δb_{rad} and δb_{pol} (c) normalized I_{sat} and D_{α} . (d) Normalized U-probe V_f fluctuations compared with divertor V_f -L39 and V_f -L1. (e) Cross-field pattern hodogram described by the δb_{rad} and δb_{pol} fluctuations during the same time window, color code follows the time evolution of the corresponding δJ_{tor} . (For interpretation of the references to colour in this figure legend, the reader is referred to the web version of this article.)

of multiple peaks for each event in Fig. 3, provides a picture of an ELM density feature composed by multiple fragmented structures, rather than a single one and those structures are evolving in time. The typical time window for the most apparent ELM manifestation, at the probe location, is of the order of $\sim 200 \mu\text{s}$.

4.2. ELM electromagnetic features

The Fig. 5 showed the details of the density structure fragments associated to a single ELM. As a further step the detailed features of a single ELM as revealed by both magnetic and electrostatic quantities measured by the COMPASS U-probe are shown in Fig. 6. The ELM time window was chosen assuming as reference the time evolution of the ELM related burst in I_{sat} signal, accordingly to the results shown in Figs. 3 and 4. In Fig. 6c and d the time behavior of locally measured I_{sat} and V_f are shown. Data are normalized to their respective maximum to make easier the comparison. Multiple structures are evident both on I_{sat} as already stated, but on the V_f as well. In particular the V_f time evolution exhibits positive and negative peaks oscillations and in this specific case three major oscillations can be recognized. The time behavior of the fluctuations of the cross-field components of magnetic field, δb_r and δb_p , as measured by one of the 3-axial coils, is shown for the same time window in Fig. 6b. Three periodic oscillation with variable intensity are observed, with a phase-shift between δb_r and δb_p in the range from $\pi/4$ and $\pi/2$. The corresponding parallel current den-

sity estimate, δJ_t , is than provided in Fig. 6a. A main peak of about 50 kA/m^2 , is detected in δJ_t and also for this quantity an oscillation between positive and negative peaks is visible. It can be noticed that the ELM related parallel current signal is composed by multiple peaks, both positive and negative and the total integral within the ELM time window is nearly zero. This behavior could be interpreted as a total current path within the ELM bunch closing along the multiple structures itself. A further detail can be captured by plotting the hodogram of the components δb_r and δb_p , Fig. 6e. The picture is obtained in the same time window of the graphs on figures 6a-d and describes the pattern of the cross-field magnetic field components at the ELM occurrence. Ideally for a simple single homogeneous monopolar current filament this pattern is expected to be closed circular. Color code in Fig. 6e follows the corresponding time evolution of δJ_t , highlighting how the elliptically shaped patterns are related to the major peaks occurrence in the δJ_t . The ELM hodogram then describes a rich and complex structure with closed pattern as a whole, indicating current filaments elongated along the main magnetic field within the ELM bunch. So that beside a composite electrostatic structure also a composite filamentary current density structure is associated to ELM bursts.

As a matter of comparison the corresponding ELM peak detected in the D_{α} signal is shown in Fig. 6c, evidencing a wider peak with respect to the local measurements provided by the probe. This different behavior is likely related to a less localized and line integrated feature of D_{α} signal. A time delay is observed with re-

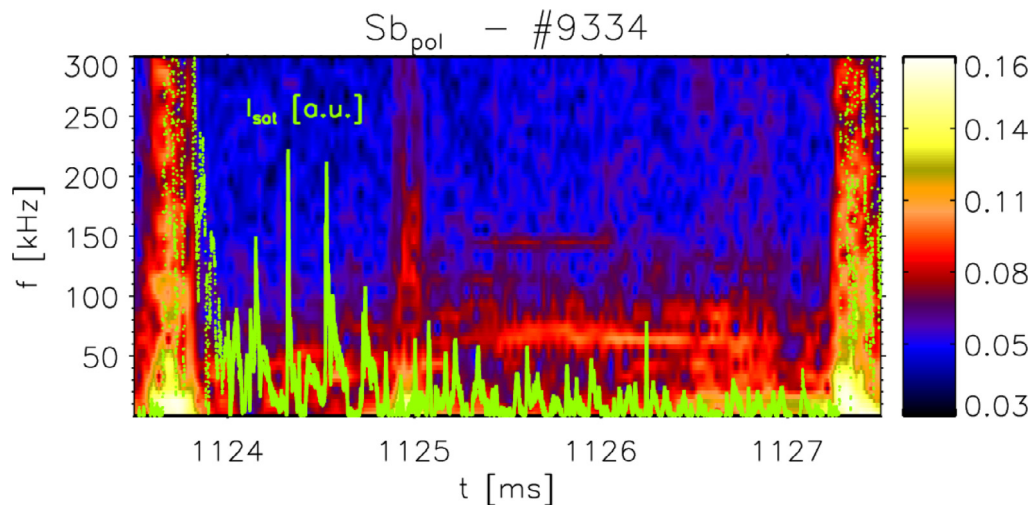


Fig. 7. Spectrogram of the δb_{pol} during an inter-ELM phase, the corresponding local I_{sat} time evolution (green continuous line) is over-plotted in a.u. (For interpretation of the references to colour in this figure legend, the reader is referred to the web version of this article.)

spect to the probe signals, likely due to the different location in the COMPASS machine.

It is interesting to note also the detailed comparison with Langmuir probe measurements in the divertor plate (Fig. 6d). In particular a very similar time behavior is observed between V_f measurement on the U-probe location and the V_f measured on the divertor probe L39, located on the field line connected with the U-probe. In particular the first strong positive ELM related peak is observed in both signals. On the other side larger differences are observed instead with the probe L1 on the opposite side of divertor and not connected to the U-probe.

The ELM burst revealed in different machine positions along the same field line and in particular on the divertor, supports the picture of the ELM filamentary structure is elongated along the field line and the hypothesis of a circuit pattern closing along the magnetic field line through the divertor sheath. This picture is consistent with the current filament circuit scheme in the SOL proposed by Krasheninnikov [22]. Analogous results are obtained in the study on 3D features of turbulent EM filaments in SOL [11].

5. Inter-ELM structures

The phase in between ELMs is populated as well by structures but with a shorter time scale. As an example one inter-ELM phase is provided in Fig. 7. The frame includes also the two adjacent ELM bursts for a better identification of the inter-ELM time window. With an increased detail with respect to the Fig. 3, the spectrogram of the δb_{pol} is provided and as a reference for bursty events the I_{sat} signal is over-plotted in green. The magnetic related sawtooth activity, see Section 3, is now apparent in the spectrum peak at $t \sim 1125$ ms. The mode at 50–70 kHz is present continuously from $t = 1125$ ms onward. In the phase immediately after the ELM this magnetic activity is absent and later on starts to appear with increasing intensity up to the phase closely preceding the next one ELM. In the phase preceding ELM the presence of discrete mode is revealed (Fig. 7), characterized by discrete frequencies up to 150 kHz, within the explored range.

The investigation of the electromagnetic features of structures was focused in this phase where the mode 50–70 kHz does not dominate the magnetic fluctuations. As can be deduced through the comparison with the Fig. 3, these I_{sat} events are by far smaller than the ELM related ones, however this zooming on inter-ELM phase allow appreciating their bursty behavior. Fig. 8 shows the fluctuations time behavior during 0.5 ms in the inter-ELM phase of

δJ_{tor} , and of δI_{sat} and δV_f , the latter ones normalized to their maximum value. The I_{sat} bursts are associated also in the inter-ELM phase to bipolar, generally asymmetric, structures in δV_f . Strong fluctuations are also observed in the δJ_{tor} . As a further detail the right column of Fig. 8 shows the time evolution of a single density burst. Resulting associated with a peak and valley of δV_f and a peak of parallel current density fluctuation, of about 0.65 kA/m^2 , indicative of the presence of a EM filamentary structure, developed on a time scale of the order of tens of microseconds. It can be concluded that the inter-ELM structures studied exhibit features similar to the ELM, but characterized by a more that one order of magnitude smaller in amplitude and time scale.

6. Discussion and conclusions

The ELM events obtained during H-mode NBI assisted COMPASS discharges were clearly detected in the SOL region and investigated in detail by the COMPASS U-probe, from the point of view of their electrostatic and magnetic properties.

In the inter-ELM phase a discrete magnetic activity onset around 50–150 kHz was observed to precede the ELM occurrence. Quasi coherent magnetic and electrostatic modes were observed in the so called D_α H-mode in Alcator C-mod [23] and measured in the proximity of the LCFS, where the electrostatic mode are detected within the first 5 mm from the LCFS. The lack of the clear electrostatic counterpart in the present case could be due to its different radial location from the LCFS, $\Delta r_{\text{LCFS}} \geq 40$ mm. The behaviour of modes preceding the ELM onset and disappearing after the ELM crash was observed in Alcator C-Mod [24] and DIII-D [25], in this latter case with frequencies in the same range observed in Figs. 3 and 7. Also in those cases, where the consistency with kinetic ballooning modes was deduced, the localization near the LCFS is indicated as important and modes are observed in both magnetic and electrostatic quantities. Further experiments are envisaged to disentangle this issue. Work is in progress also to investigate the relationship of the shown electromagnetic measurements in the SOL with the edge Mirnov coil measurements on the COMPASS vessel, where ballooning modes were identified during H-mode [26].

ELM features are identified as strong burst of density and generally dipolar structures in V_f potential. A local electron temperature measurement would help in completing the electrostatic picture; however these findings are not expected to change significantly for the plasma potential according to the temperature esti-

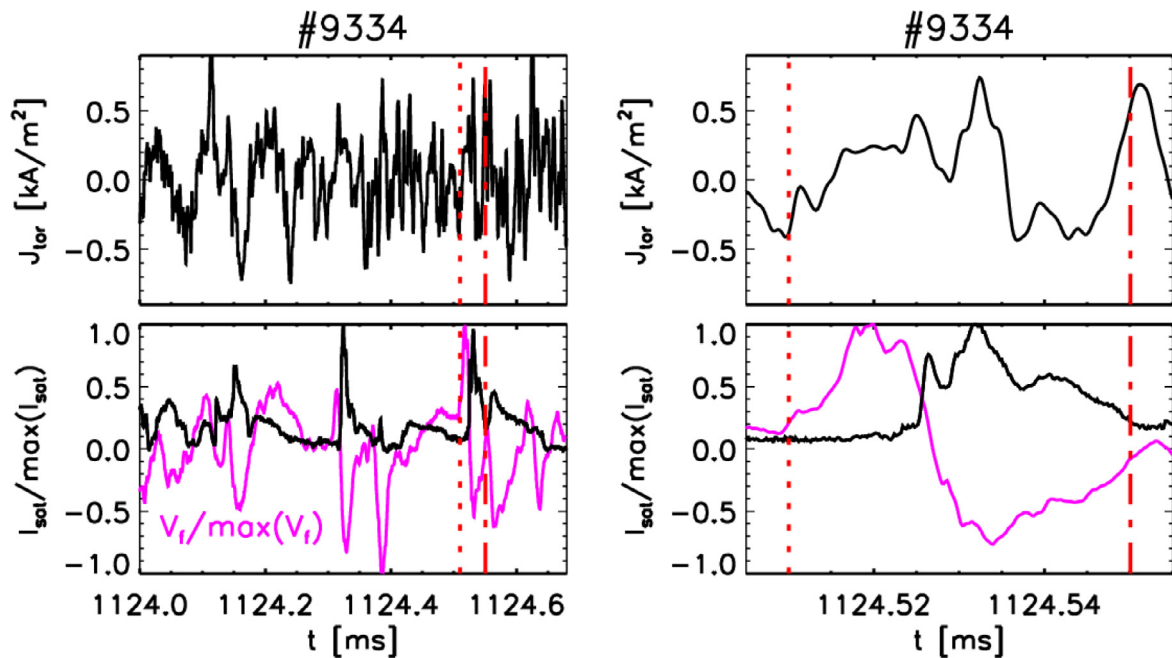


Fig. 8. Time evolution during about half ms of an inter-ELM phase of δJ_{tor} , and of δI_{sat} and δV_i normalized to their maximum value fluctuations (left column). Detail on the same quantities zooming on a single event detected on δI_{sat} in the inter-ELM phase. Vertical dashed lines highlight the corresponding time instants on the left and right panels. (For interpretation of the references to colour in this figure legend, the reader is referred to the web version of this article.)

mate shown in [18]. Thanks to the high time and space resolution of the COMPASS U-probe their fine composite structure was revealed, consisting in multiple fragmented smaller structures rather than a single larger one. The EM features were investigated in the cross-field plane providing a clear fingerprint of filamentary EM structures, constituted by multiple parallel current density filament associated to one single ELM occurrence. Both positive and negative peaks are detected indicating the consistency of a return current pattern within the filament bunch itself. This observation is in agreement to the equivalent circuit model proposed for the EM filaments in the SOL [20], which foresees the closure pattern via the limiter sheath. Along this line another interesting observation is represented by the correlation observed on one single ELM monitored on V_i along the same field line on the divertor region, confirming its elongated structure along the field line up to the divertor. The total balance of the filament circuitation in the SOL and divertor sheath would deserve a further statistical investigation. In the case studied in this paper an ELM filament current density of the order of 50 kA/m^2 was observed. On the other hand the inter-ELM features were investigated as well. It can be concluded that the inter-ELM structures studied exhibits features similar to the ELM, but characterized by a more than one order of magnitude smaller in amplitude and time scale. The detected magnetic fluctuations associated to ELM are much lower than the equilibrium $B_t = 1.15 \text{ T}$ and poloidal magnetic field at the probe location ($\sim 0.2 \text{ T}$). So that an effective field line bending is not expected in this case. However for the ELMs the measured current density is not negligible and effects on current transport [1] can be figured out. Similar observations were obtained also for type-I ELM in ohmic H-mode discharges and work is in progress in order to perform a statistical comparison between different ELM types and H-mode regimes.

Acknowledgments

This work has been carried out within the framework of the EUROfusion Consortium and has received funding from the Eu-

ropean Union Horizon research and training programme 2014–2018 under grant agreement no. 633053 and co-funded by MEYS projects No. 8D15001 and LM2015045. The views and opinions expressed herein do not necessarily reflect those of the European Commission.

References

- [1] D.A. D'Ippolito, J.R. Myra, S.J. Zweben, *Phys. Plasmas* 18 (2011) 060501.
- [2] M. Endler, et al., *Phys. Control. Fusion* 47 (2) (2005) 219.
- [3] D.A. D'Ippolito, J.R. Myra, S.I. Krasheninnikov, *Phys. Plasmas* 9 (2002) 222.
- [4] P. Manz, et al., *Phys. Plasmas* 20 (2013) 102307.
- [5] M. Xu, et al., 24th IAEA Fusion Energy Conference, San Diego (CA), 2012 paper EX/7-Rb.
- [6] G. Tynan, et al., *Nucl. Fusion* 53 (2013) 073053.
- [7] G.S. Xu, V. Naulin, W. Fundamenski, J.J. Rasmussen, et al., *Phys. Plasmas* 17 (2010) 022501.
- [8] N. Vianello, et al., *Phys. Rev. Lett.* 106 (2011) 125002.
- [9] M. Spolaore, et al., *Phys. Rev. Lett.* 102 (16) (2009) 165001.
- [10] I. Furno, et al., *Phys. Rev. Lett.* 106 (24) (2011) 245001.
- [11] K. Kovarik, et al., in: 41st EPS Conference on Plasma Physics, Berlin, Germany, 2014, p. P5.025.
- [12] M. Spolaore, et al., *Phys. Plasmas* 22 (2015) 012310.
- [13] R. Panek, et al., *Phys. Control. Fusion* 58 (2016) 014015.
- [14] J.A. Van Allen, *Am. J. Phys.* 74 (2006) 809.
- [15] M. Spolaore, N. Vianello, M. Agostini, R. Cavazzana, E. Martines, G. Serianni, P. Scarin, E. Spada, M. Zuin, V. Antoni, *J. Nucl. Mater.* 390 (2009) 448–451.
- [16] C.G. Silva, et al., *Contrib. Plasma Phys.* 38 (2010) S1.
- [17] M. Dimitrova, et al., *Contrib. Plasma Phys.* 54 (2014) 255–260.
- [18] J. Adamek, et al., *Nucl. Fusion* 57 (2017) 022010.
- [19] A. Leonard, *Phys. Plasmas* 21 (2014) 090501.
- [20] Y. Liang, Edge localized mode (ELM), in: *Active Control of Magneto-Hydrodynamic Instabilities in Hot Plasmas*, Springer Berlin Heidelberg, 2015, pp. 143–181.
- [21] Y. Sechrest, et al., *Nucl. Fusion* 52 (2012) 123009.
- [22] S.I. Krasheninnikov, D.A. D'Ippolito, J.R. Myra, *J. Plasma Phys.* 74 (2008) 679–717.
- [23] J.A. Snipes, et al., *Plasma Phys. Control. Fusion* 43 (2001) L23–L30.
- [24] A. Diallo, et al., *Phys. Rev. Lett.* 112 (2014) 115001.
- [25] A. Diallo, *Phys. Plasmas* 22 (2015) 056111.
- [26] A. Melnikov, et al., *Plasma Phys. Control. Fusion* 57 (2015) 065006.